

Cyclotron absorption of radio emission within pulsar magnetospheres

Qinghuan Luo[★] and D. B. Melrose

Research Centre for Theoretical Astrophysics, School of Physics, University of Sydney, NSW 2006, Australia

Accepted 2001 February 6. Received 2001 February 6; in original form 2000 December 18

ABSTRACT

Absorption of radio emission through normal cyclotron resonance within pulsar magnetospheres is considered. The optical depth for cyclotron damping is calculated using a plasma distribution with an intrinsically relativistic spread. We argue that such a broad distribution is plausible for pulsar plasmas and that it implies that a class of pulsars that should have cyclotron damping extends to include young pulsars with shorter periods and stronger magnetic fields. There is no obvious observational evidence for disruption of radio pulses, which implies that the optical depth cannot be too large. We propose that cyclotron resonance may cause marginal absorption of radio emission. It is shown that such marginal absorption produces potentially observable asymmetric features for double-peak pulse profiles with wide separation, with one peak tending to be suppressed.

Key words: acceleration of particles – radiation mechanisms: non-thermal – pulsars: general.

1 INTRODUCTION

The mechanism for pulsar radio emission is not well understood (for a review cf. Melrose 2000). Observations suggest that the emission is produced well inside the light cylinder (which is defined as the radial distance at which the rotation speed equals the speed of light), in the strong magnetic field region with the relevant radio frequency being much lower than the cyclotron frequency (e.g. Blaskiewicz, Cordes & Wasserman 1991). Generally, the pulsar magnetic field can be adequately modelled as a magnetic dipole with the field strength decreasing rapidly with the radial distance as $B \propto 1/R^3$. Thus, radio waves with frequency ω must propagate through a transition region from $\Omega_e \gg \omega$ to $\Omega_e \leq \omega$, where Ω_e is the electron cyclotron frequency. This transition region can be located well inside the light cylinder (LC) for some pulsars. In this transition region, the magnetic field becomes sufficiently weak so that in the rest frame of the electron the relevant wave frequency is equal to the cyclotron frequency. The cyclotron resonance can cause waves to damp.

Cyclotron damping has been discussed by several authors (e.g. Blandford & Scharlemann 1976; Mikhailovskii et al. 1982; Lominadze et al. 1986; Kazbegi et al 1991; Lyubarskii & Petrova 1998). So far there is no definitive answer as to whether the damping effect is important for pulsar radio emission. The cyclotron resonance condition can be satisfied at least for some typical pulsars if not for all. If the resonance can lead to some observational signature, the known pulsars could be separated into two distinct groups: one group with cyclotron damping and the other without cyclotron damping. Effective cyclotron damping would affect the polarization of the pulsar radio emission, as

cyclotron resonance causes preferential absorption of waves with a particular type of polarization, which ought to be observable. However, there appears to be no obvious observational evidence for the separation of pulsars into two groups based on polarization. The observed polarization features, such as circular polarization and orthogonal mode switch, occur more or less uniformly for pulsars distributed in the $P-\dot{P}$ diagram (Han et al. 1998; Gould & Lyne 1998). The lack of evidence for disruption of the radio emission as a result of cyclotron absorption implies either that the cyclotron resonance has no effect at all on the radio emission or that the resonance causes only marginal absorption. In the latter case, the radio emission experiences cyclotron absorption but can still escape from the magnetosphere.

The early studies of cyclotron damping assumed a plasma that is non-relativistic in its rest frame. The possibility of a broad distribution for pulsar plasmas was considered by Daugherty & Harding (1983), Arons & Barnard (1986) and others (e.g. Weatherall 1994; Gedalin, Melrose & Gruman 1998; Melrose & Gedalin 1999). A broad distribution seems to be plausible for the secondary pair plasma given broad range of dynamics of an e^\pm pair cascade (e.g. Daugherty & Harding 1983) and possible re-acceleration of secondary pairs by unscreened electric fields (Shibata, Miyazaki & Takahara 1988). Inclusion of the relativistic effect gives rise to variety of new features of wave dispersion (Melrose & Gedalin 1999; Kennett, Melrose & Luo 2001, hereafter KML). One such new feature, which is not well understood, is the possible modification of wave absorption as a result of cyclotron resonance.

The purpose of this paper is to discuss the conditions for cyclotron damping within the pulsar magnetosphere. In particular, we calculate the optical depth for cyclotron damping with an intrinsically relativistic distribution. The result is compared to the

[★]E-mail: luo@physics.usyd.edu.au

non-relativistic case. Two mechanisms that can broaden the secondary pair distribution are discussed. These are the broadening as a result of (1) an asymmetric energy distribution between members of a pair as a result of the near threshold effect and (2) re-acceleration of secondary pairs by an unshielded electric field. We discuss possible observational effects that come from marginal cyclotron absorption in which radio emission is subjected only to minor absorption and is able to escape from the magnetosphere. Throughout our discussion we assume the strong magnetic field approximation, in which particles are in their ground state (lowest Landau level). Cyclotron absorption is assumed to involve only transitions from the ground state to the first Landau level.

2 ABSORPTION AS A RESULT OF CYCLOTRON RESONANCE

In the strong pulsar magnetic field, the cyclotron resonance is $\omega - k_{\parallel}v_{\parallel} \pm \Omega_e/\gamma = 0$, where \pm correspond respectively to the anomalous and normal cyclotron resonances, k_{\parallel} is the parallel (to the magnetic field lines) wavevector and v_{\parallel} is the parallel velocity. We assume a uniform magnetic field. As pulsar magnetic field lines are curved, this assumption is valid only for particles with a modest Lorentz factor, otherwise curvature drift needs to be included (e.g. Kazbegi et al. 1991). The anomalous cyclotron resonance (ACR) can lead to cyclotron instability, and the normal cyclotron resonance (NCR) gives rise to wave damping. Given ω and Ω_e , for cyclotron resonance to occur the particle's velocity $v = \beta c$ must satisfy the following condition:

$$\beta_{\pm} = \frac{\omega k_{\parallel} c \pm \Omega_e (\Omega_e^2 + k_{\parallel}^2 c^2 - \omega^2)^{1/2}}{\Omega_e^2 + k_{\parallel}^2 c^2} = \frac{z \pm y(1 + y^2 - z^2)^{1/2}}{1 + y^2}, \quad (1)$$

where $z = \omega/k_{\parallel}c$, and $y = \Omega_e/k_{\parallel}c$. The corresponding Lorentz factor is $\gamma_{\pm} = 1/\sqrt{1 - \beta_{\pm}^2} = [|yz \pm (1 + y^2 - z^2)^{1/2}|/(z^2 - 1)]$. Note that z can be interpreted as the parallel phase speed of the relevant waves. NCR is allowed in both subluminal and superluminal regions, $z \leq 1$ and $1 \leq z \leq (1 + y^2)^{1/2}$, while ACR is allowed only in the subluminal region $z < 1$.

2.1 Normal cyclotron resonance

Damping as a result of NCR occurs when the doppler-shifted frequency in the particle rest frame matches the cyclotron frequency. Let θ be the angle between the wave normal direction and the tangent to the magnetic field line, which is also the direction of the particle motion. So we have $k_{\parallel} = k \cos \theta$. There is a critical angle $\theta_0 = 1/\gamma$ where γ is the particle's Lorentz factor: for $\theta < \theta_0$ the wave frequency is redshifted in the rest frame of the particle and for $\theta > \theta_0$ the frequency is blueshifted. In the pulsar magnetosphere, we assume the bulk plasma streams outwards along the open field lines. For convenience, the pulsar frame is used.

In the small angle case, for $z \leq 1$ NCR is possible only for waves with sufficiently high frequency $\omega > \Omega_e$ (Lominadze et al. 1986; Kazbegi et al. 1991). The resonant particles must have velocity β_- given by equation (1). For $\omega \gg \Omega_e$, more specifically, $y \ll 1$ and $y^2 \gg 1 - z^2$, and from equation (1) we have

$$\beta_- \approx \frac{1 - y^2}{1 + y^2} \approx 1 - 2y^2, \quad \gamma_- \approx \frac{1}{2y} \gg 1. \quad (2)$$

In general, the condition $\omega \gg \Omega_e$ cannot be satisfied within the LC except for a very small number of slow pulsars.

However, if particles are allowed to have negative velocity, e.g. particles from a return flux, NCR can occur for low-frequency waves with $\omega \ll \Omega_e$. Specifically, for $y \gg 1$, particles in NCR have negative velocity $\beta_- < 0$, given by (1). Assuming $y^2 \gg |z^2 - 1|$, we obtain

$$\beta_- \approx -1 + \frac{1(1+z)^2}{2(1+y^2)}, \quad \gamma_- \approx \frac{1}{2}y \gg 1, \quad (3)$$

where the approximation for γ_- is made for $y \gg 1$ and $z \approx 1$.

For $\theta > \theta_0$, because particles see the blueshifted frequency, NCR is possible for low frequency waves $\omega \ll \Omega_e$ with $1 \leq z \leq (1 + y^2)^{1/2}$. In particular, waves with $0 < z - 1 \ll 1$ can be damped by particles with $\beta_+ > 0$ and large γ_+ given by

$$\beta_+ \approx 1 - \frac{1(1-z)^2}{2(y^2 + 1)}, \quad \gamma_+ \approx \frac{y}{z-1}. \quad (4)$$

The NCR condition is shown in Fig. 1. For NCR to occur in the low frequency region $\omega \ll \Omega_e$, one requires that the resonant particles have a large Lorentz factor and that the waves have dispersion $z > 1$ corresponding to a large propagation angle. For pulsars, this case is particularly relevant; pulsar magnetic field lines are curved, causing the radio waves to acquire a substantial angle relative to the field line direction. Moreover, the waves with initially $z < 1$ and $\theta = 0$ develop a parallel phase speed $z > 1$ as θ increases (KML). In Section 3, it is shown that the condition (4) is appropriate for NCR inside the LC.

2.2 Anomalous cyclotron resonance

ACR can only occur for waves with $z < 1$, and only for the particles that have positive velocity $\beta_+ > 0$ (relative to forward propagating waves). For $y^2 + 1 \gg |1 - z|$, we obtain β_+ and γ_+ , given by the same expressions as (4). Note that $\gamma_+ \gg 1$ for $y^2 + 1 \gg (1 - z)^2$. Only those energetic particles with $\gamma_+ \gg 1$ can satisfy ACR (e.g. Kazbegi et al. 1991; Lyutikov, Blandford & Machabeli 1999). The ACR condition is shown in Fig. 2. ACR is only allowed in the region $z < 1$. Particles with a velocity given by

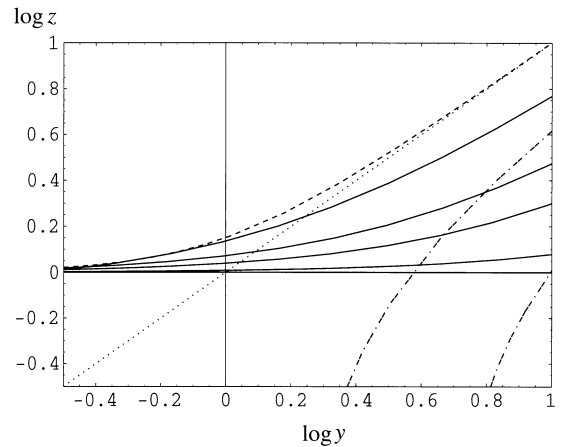


Figure 1. The parameter regime of cyclotron damping. The dashed curve and horizontal line correspond respectively to $z = (1 + y^2)^{1/2}$ and $z = 1$. The four solid curves from top to bottom represent NCR by forward moving electrons with $\gamma = 2, 5, 10,$ and 50 . The dash-dot curves correspond to resonance by backward moving electrons with $\gamma = 2$ and 5 .

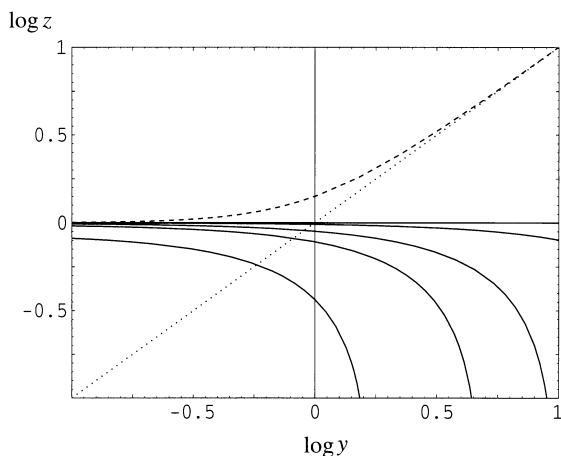


Figure 2. As in Fig. 1 with the four solid curves corresponding to ACR with $\gamma = 50, 10, 5, 2$ (from top to bottom). The resonance occurs only within the region $z < 1$. For waves with dispersion $0 < 1 - z \ll 1$ to have ACR instability in the low frequency region $\omega \ll \Omega_e$, electrons need to have very large Lorentz factors $\gamma \gg 1$ so that resonance curves are able to approach $z = 1$ at large y .

equation (4) can have NCR or ACR, but the two types of resonance cannot occur in the same location (because both $z > 1$ and $z < 1$ cannot be satisfied at the same time).

2.3 Absorption coefficient

In general, dispersion of various wavemodes can be obtained by calculating the permittivity tensor, \mathbf{K}_{ij} . From the permittivity tensor one can calculate the absorption coefficient for a given wavemode. A general formula for the absorption coefficient is given in Appendix A.

Possible low-frequency wavemodes in non-gyrotropic plasmas in the $\beta_A = v_A/c = \langle v/c \rangle^{-1/2} \Omega_e/\omega_p \gg 1$ (where v is the particle velocity) limit were discussed in detail in KML. To emphasize cyclotron damping we consider a quasi-neutral plasma, for which the permittivity tensor is simplified considerably by ignoring the non-gyrotropic terms. In this approximation, together with the strong magnetic field limit, the dispersion equation factorizes into two equations, with one describing the X mode (t mode or the magnetoacoustic mode) and the other describing the L–O mode, which includes, as limiting cases, the Langmuir mode (parallel propagation), the O mode and the Alfvén mode.

As a working hypothesis it is assumed that radio emission can be expressed in terms of X mode (purely transverse mode) and L–O mode (quasi-transverse). We do not consider the propagation effect such as refraction caused by the plasma. The region of interest is then relatively far away from the polar cap (PC) and also perhaps from the location where emission is produced.

For the X mode the polarization vector is $\mathbf{e}_X = (0, i, 0)$, so that the only relevant component of the dielectric tensor is \mathbf{K}_{22} (e.g. Lominadze et al. 1986; Kazbegi et al. 1991; Melrose & Gedalin 1999; KML). One may derive the antihermitian components by considering the cyclotron resonance terms only. For NCR, only terms with $\delta(\omega - k_{\parallel}v_{\parallel} - \Omega_e/\gamma)$ are relevant.

Considering waves with $z > 1$ in NCR with particles with γ_+ given by equation (4), the absorption coefficient is obtained as (Appendix A)

$$\Gamma_X = \pi \frac{\omega^2}{\omega} F(u_+), \quad (5)$$

where $F(u_+)$ is the plasma density and $u_+ = \beta_+ \gamma_+$. In deriving (5) we assume $\ln |n - 1| \ll \theta^2/2 \ll 1$ and $\gamma_+ = 2\Omega_e/\omega\theta^2$, where θ is the propagation angle relative to the magnetic field.

For the L–O mode the polarization vector is $\mathbf{e}_{L-O} = (e_1, 0, e_3)$. As \mathbf{K}_{11}^A is identical with \mathbf{K}_{22}^A , for $\theta \ll 1$, we have $\Gamma_{L-O} \approx \Gamma_X$, that is, for parallel propagation, both X and L–O modes have the same damping rate. For oblique propagation for L–O mode one has $|e_1/e_3|^2 < 1$. The dominant terms with the cyclotron resonance are \mathbf{K}_{11}^A and \mathbf{K}_{13}^A and as a result the absorption coefficient for the L–O mode is different from that for the X mode. However, for a sufficiently underdense plasma, with the plasma frequency being much lower than the wave frequency, the difference becomes insignificant and is neglected here.

3 CYCLOTRON DAMPING INSIDE THE LIGHT CYLINDER

Observations suggest that for most pulsars the radio emission is produced well inside the LC (e.g. Blaskiewicz et al. 1991). A pulsar magnetosphere is probably populated with a dense pair plasma produced by cascades above the PC. However, simple estimates suggest that the resulting plasma is too dense to allow escape of the radiation. Nevertheless, there must be a way that the radio emission is able to propagate out to the outer magnetospheric region. One suggestion is that the magnetospheric plasma is spatially inhomogeneous, consisting of many underdense regions. The radio emission is ducted out from the inner magnetosphere through these underdense structures (Melrose 2000). Another possibility is that smoothly varying inhomogeneity such as the plasma density or magnetic field causes the rays to bend to follow curved field lines (Melrose 1979; Barnard & Arons 1986; McKinnon & Stinebring 1998). The ray-tracing study by several authors, e.g. Barnard & Arons (1986), showed that propagation of the L–O mode waves follows curved field lines while X-mode waves propagate nearly along straight lines. Barnard and Arons’ result for the X mode was based on the assumption that the X-mode dispersion is approximated by $n = 1$, precluding any refraction. When this condition is relaxed, the X-mode waves experience some refraction as a result of any gradient in the Alfvén speed. As the waves propagate outward, the plasma density decreases. One may define a characteristic radial distance beyond which the wave polarization and propagation trajectory are no longer significantly affected by the plasma. This radius is referred to as the polarization limiting region (PLR) (e.g. Melrose 1979). Our following discussion applies only to the region above the PLR.

In the region above the PLR, the relevant waves are assumed to propagate along straight lines. As a result of the curvature of field lines, the propagation angle θ increases monotonically. (For a rotating dipole, θ is asymmetric in the magnetic azimuth, which is discussed in Section 5 and Appendix B.) In the following we show that waves propagating at a large angle experience NCR damping.

Within the pulsar magnetosphere, the NCR condition is satisfied favourably for low-frequency (i.e. $\omega < \Omega_e$) waves propagating at a large angle $\theta > \theta_0$ with the condition $\gamma_+ = 2\Omega_e/\omega\theta^2$ being satisfied (Section 2.1). In Fig. 3, this condition is plotted as dash-dotted ($\gamma = 5 \times 10^5$), dashed ($\gamma = 10^4$) and dotted ($\gamma = 10^2$) lines with $\omega/2\pi = 500$ MHz and $\theta = 0.4$. Although, in principle, the NCR condition can be satisfied for virtually all known pulsars, one requires particles with much higher Lorentz factor (than the bulk Lorentz factor) for NCR to be effective for fast, very young pulsars and some fast millisecond pulsars (MSPs). The population of particles with energy much higher than that of the average bulk

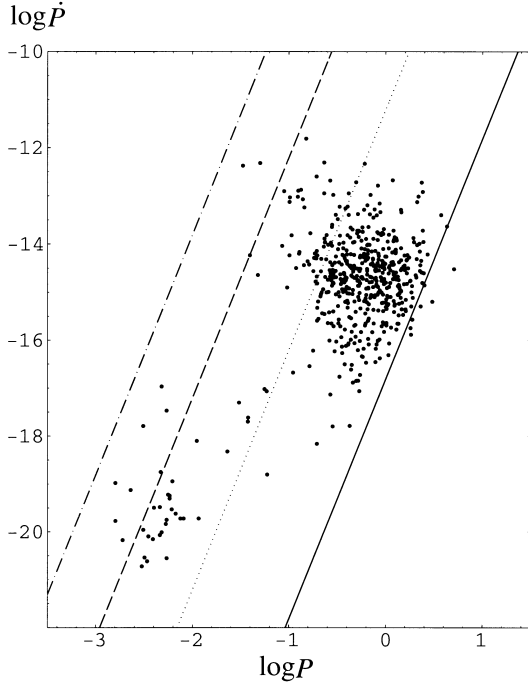


Figure 3. Cyclotron resonance condition on the period, period-derivative plane for a sample of 701 pulsars. The sample is from the Princeton pulsar catalogue (<http://pulsar.princeton.edu/pulsar/catalog.shtml>). The dash-dotted, dashed and dotted lines correspond to $\omega/2\pi = \Omega_e/\pi\theta^2\gamma = 500$ MHz with $\gamma = 5 \times 10^5$, 10^4 and 10^2 respectively, where $\theta = 0.4$ and $R = 0.8R_{LC}$. Each line separates the pulsars into two distinct groups (with NCR and without NCR). Cyclotron resonance occurs inside the radius $R = 0.8R_{LC}$ for pulsars located on the right-hand side of the line. The solid line is plotted with $\omega/2\pi = \gamma\Omega_e/\pi$, with $\gamma = 20$ and with $R = 0.8R_{LC}$.

plasma is small, and hence NCR damping may not be severe for these pulsars.

For cyclotron damping to be important, one requires the optical depth for damping exceed unity:

$$\tau = \int \frac{\Gamma}{c} ds = \pi M \int_0^s \frac{\omega_p^2}{\omega c} F\left(\frac{2\Omega_e}{\omega\theta^2}\right) ds' > 1, \quad (6)$$

where integration is along the ray path s , equation (5) for the X mode is used, M is the pair multiplicity, $\omega_p^2 = 4\pi e^2 n_{GJ}(s)/m$, n_{GJ} is the local Goldreich–Julian (GJ) density as a function of s and $\gamma_+ = 2\Omega_e/\omega\theta^2$ is assumed in the distribution $F(u)$.

Given a frequency, ω , and the Lorentz factor of a particle γ , one may define a radial distance, R_c , where cyclotron resonance occurs. Assuming θ to be a constant near the resonance region, we have $\rho_c = R_c/R_{LC} = \Theta_d^2(2\Omega_e/\omega\theta^2)^{1/3}$ where Ω_{e*} is the cyclotron frequency on the PC, $\Theta_d = (R_*/R_{LC})^{1/2}$ is the opening angle of the PC, and R_{LC} is the LC radius. For a monoenergetic distribution, one has

$$\tau = (\pi/3)M\rho_c\theta^2, \quad (7)$$

which is similar to the result in e.g. Lyubarskii & Petrova (1998). Notice that the energy distribution of secondary pairs produced through a cascade above the PC can be very broad. A broad relativistic distribution can strongly modify the cyclotron absorption.

4 A BROAD (RELATIVISTIC) DISTRIBUTION OF ELECTRON–POSITRON PAIRS

The distribution of secondary pair plasmas can be broadened due to either the broad dynamic range of photons decaying into pairs or reacceleration of secondary pairs by unscreened electric fields. Pair production through single photon decay in strong magnetic fields can be characterized by a parameter

$$\chi = 0.5\varepsilon_\gamma\varepsilon_B \sin \theta_{\gamma B}, \quad (8)$$

where $\theta_{\gamma B}$ is the propagation angle of pair-producing photons relative to the field-line direction, ε_γ is the photon energy, $\varepsilon_B = B/B_c$ is the cyclotron energy (ε_γ and ε_B are in units of the rest mass energy). For a photon to decay into a pair, apart from the minimum energy threshold $\varepsilon_\gamma \geq 2$, χ must be larger than a certain value. For pulsar parameters, we have $\chi_{\min} \approx 1/15$.

A broad energy spectrum of secondary pairs was suggested by Daugherty & Harding (1983) who calculated numerically the energy distribution between the members of a secondary pair and showed that the distribution can be characterized by the χ -value at production. For small $\chi \ll 1$, the distribution is narrowly peaked at $0.5\varepsilon_\gamma$, i.e. evenly shared by the two members. For increasing χ , the distribution broadens and when χ is sufficiently large one member of the pair can take on the major fraction of the photon energy while the other has only the rest mass energy in the $\theta_{\gamma B} = \pi/2$ frame (Daugherty & Harding 1983).

Recent studies (Shibata et al. 1998) showed that the parallel electric field may not be completely screened out by secondary pairs. This leads to the strong possibility that secondary pairs can be accelerated or decelerated, thereby broadening the distribution (e.g. Weatherall 1994).

As the first example of a broad distribution, consider a water-bag distribution (Arons & Barnard 1986):

$$F(u) = \frac{1}{u_{\max} - u_{\min}} \quad \text{for } u_{\min} \leq u \leq u_{\max}, \\ = 0 \quad \text{otherwise.} \quad (9)$$

The upper and lower cut-offs of the distribution define two radial distances, R_{\min} and R_{\max} , by $\gamma_{\max} = 2\Omega_e(R_{\min})/\omega\theta^2$ and $\gamma_{\min} = 2\Omega_e(R_{\max})/\omega\theta^2$, respectively. For $R_{\max}/R_{LC} \leq 1$, the optical depth (equation 6) can be evaluated analytically using equation (9), giving

$$\tau = \frac{\pi}{2}\theta^2 M \rho_{\max} \frac{\xi^{1/3}(1 - \xi^{2/3})}{1 - \xi}, \quad (10)$$

where $\xi = u_{\min}/u_{\max} \approx \gamma_{\min}/\gamma_{\max} < 1$ and $\rho_{\max} = R_{\max}/R_{LC}$ is the maximum radius within which cyclotron resonance occurs. Assuming the distribution has a spread of γ_T in the plasma rest frame, one has $\gamma_{\min} \approx \gamma_s/2\gamma_T$ and $\gamma_{\max} \approx 2\gamma_s\gamma_T$, where γ_s is the bulk plasma Lorentz factor. A monoenergetic distribution corresponds to the limit $\xi = 1$ and then equation (10) reduces to equation (7). As for a relativistic distribution we have $\xi \ll 1$, the optical depth calculated assuming the monoenergetic distribution $\gamma = \gamma_s$ overestimates the NCR effect for pulsars with parameters that satisfy $\rho_c(\gamma = \gamma_s) \leq 1$. However, because the maximum Lorentz factor is now $\gamma_{\max} \approx 2\gamma_s\gamma_T$, young pulsars with short and strong magnetic fields should have cyclotron absorption as well.

For a relativistic hot plasma, we consider the distribution in the pulsar frame

$$F(u) = N^{-1} \exp[-\varrho_T \gamma \gamma_s (1 - \beta\beta_s)], \quad (11)$$

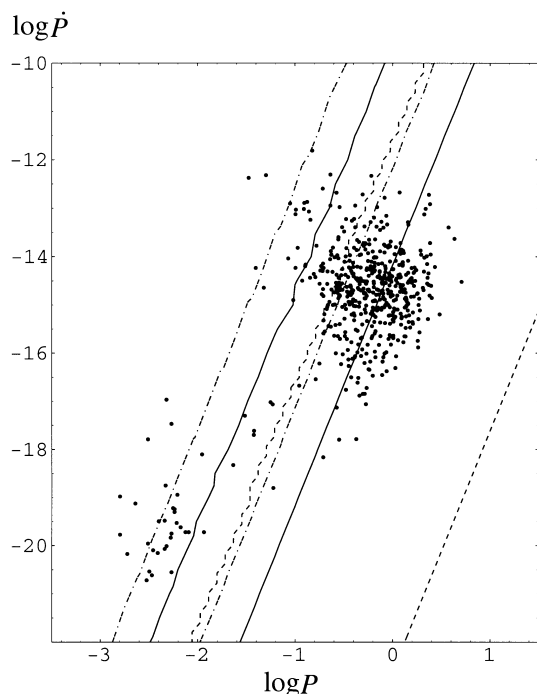


Figure 4. Pulsars with cyclotron absorption. The two solid curves are the contour plot of $\tau = 1$ for a relativistic distribution with $q_T = 0.1$, $\gamma_s = 100$. The dashed curves correspond to $\tau = 1$ for a monoenergetic distribution. The dash-dot-dashed curve corresponds to a large bulk Lorentz factor, $\gamma_s = 10^3$. We assume $M = 10^3$, $\theta = 0.2$, $\omega/2\pi = 500$ MHz.

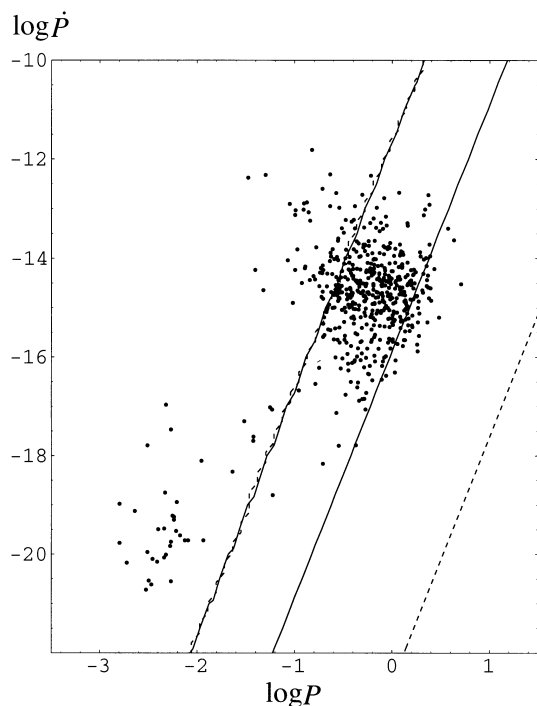


Figure 5. As in Fig. 4 for $q_T = 2$.

where $\gamma_s = 1/\sqrt{1 - \beta_s^2}$ is the bulk Lorentz factor, q_T is the inverse of temperature in $m_e c^2$, and N is the normalization factor so that $f(u)$ is normalized to unity. The optical depth, equation (6), can be calculated numerically using (11). Figs 4 and 5 show contour plots of $\tau = 1$ in the P - \dot{P} diagram for the distribution (11) with $q_T = 0.1$

and $q_T = 2$ respectively. Pulsars located within the two lines have $\tau \geq 1$. The two dashed lines correspond to the monoenergetic distribution. For a broader distribution, more pulsars with short periods and strong magnetic fields should have cyclotron absorption.

Apart from the broadness that can affect the cyclotron absorption, the damping depends strongly on the bulk Lorentz factor. The larger the value of γ_s , the more pulsars with shorter periods can have NCR. As there is no accurate way to estimate γ_s , we present here a qualitative estimate by assuming that γ_s is determined by the initial pitch angle at pair creation (Luo, Shibata & Melrose 2000). The Lorentz factor of the one-dimensional motion of a pair is given by (Luo et al. 2000)

$$\gamma_s \approx 1/\psi_0, \quad (12)$$

where ψ_0 is the initial pitch angle. For single photon decay into a pair, we have $\psi_0 \approx \theta_{\gamma B}$ with $\theta_{\gamma B}$ defined in (8). From (8) one obtains

$$\gamma_s \approx 0.5 \epsilon_{\gamma} \epsilon_B / \chi. \quad (13)$$

The critical value χ for pair production is not particularly sensitive to pulsar parameters. Thus, we may set $\chi = 1/15$, leading to a range $\gamma_s = 5-10^4$. For older pulsars and MSPs we have smaller γ_s because a relatively large $\theta_{\gamma B}$ is required for pair production, and for young, fast-rotating pulsars (with strong magnetic fields), pair production occurs at a small angle and then we have large γ_s . This result is qualitatively in agreement with the numerical simulation of pair cascading by Daugherty & Harding (1982).

In summary, cyclotron absorption appears to be important for normal pulsars and some MSPs. As shown from equations (7) and (10) and Figs 4 and 5, the optical depth can be much larger than unity for the majority of pulsars with the typical physical parameters that are widely used in polar cap models. For young pulsars, it appears to be plausible that the secondary pair plasma distribution is broader and intrinsically relativistic, with a large bulk Lorentz factor compared to typical pulsars. The distribution of pulsars that should have cyclotron absorption extends to include young pulsars with a short period and a strong magnetic field. However, because the exact form of the distribution such as the bulk Lorentz factor and the relativistic spread is not well known, the left boundary shown in Figs 4 and 5 cannot be determined completely.

The fact that pulsars can be observed implies that cyclotron absorption does not completely destroy radio pulses. One possibility is that radio emission is only marginally absorbed through NCR (with the optical depth close to or less than 1). One may have small or moderate optical depth if the escaping radio emission propagates in the underdense region with plasma density less than the Mn_{GJ} .

5 PULSE PHASE ASYMMETRY IN ABSORPTION

We consider those pulsars that should experience cyclotron absorption and discuss the likely observational effects. Here we discuss specifically the possibility of marginal absorption and suggest that cyclotron absorption is asymmetric with respect to the magnetic pole, which produces pulse-phase dependent cyclotron absorption. This asymmetry should be observable for those pulsars with double-peak pulse profiles.

5.1 Asymmetric propagation angle

For a rotating dipole, the rotation introduces modification to the propagation angle θ as a result of aberration and field line sweep-back. When the inclination angle is not zero, these effects lead to asymmetry of the propagation angle in the magnetic azimuth. The field line sweep-back is a small effect well inside the light cylinder, being of order $(R/R_{LC})^2$ (e.g. Shitov 1985; Barnard 1986). We concentrate here on the consequences of aberration.

We assume a ray starts at \bar{x} in the direction \bar{b} . The geometry of a rotating dipole is shown in Fig. 6. In the region above the PLR, the ray propagates along a straight line. After Δt , the ray propagates a distance in units of the LC radius, $s = c\Delta t/R_{LC}$, and reaches x crossing field lines with a tangential vector b at x . Then the propagation angle is given by

$$\cos \theta = \bar{b} \cdot b. \quad (14)$$

To obtain b , consider a point x' on the rotation trajectory which passes through x , and assume that at Δt the point x' moves to x as the dipole rotates an angle $\Delta\Psi = \Omega\Delta t = s$. Let b' be the tangential vector of the field line at x' . In the magnetic polar coordinates, we have $b' = (e_{R'} \cos \Theta' + e_{\Theta'} \sin \Theta'/2)/A$ where $A = [1 - (3/4)\sin^2 \Theta']^{1/2}$ and (R', Θ', Φ') are the polar coordinates of x' , and where $e_{R'}$, $e_{\Theta'}$ and $e_{\Phi'}$ are the polar unit vectors. One can obtain b by rotating b' from x' to x by an angle $\Delta\Psi = s$. A general form of b is given by equation (B16) in Appendix B. In general, a rotating dipole magnetic field is not axisymmetric, the exception being for an aligned rotator. Hence, b depends on the magnetic azimuth and the propagation angle θ is asymmetric about the magnetic axis.

The initial propagation direction, \bar{b} , is assumed to be in the bulk plasma flow direction at the point of emission. The plasma rotates with velocity $\Omega \times R$, and the radio emission is then beamed in the direction (e.g. Blaskiewicz et al. 1991; Hibschan & Arons 2001; Appendix B of this paper),

$$b_v = b_0 + \rho[\hat{\Omega} \times \hat{\rho} - (\hat{\Omega} \times \hat{\rho}) \cdot b_0 b_0], \quad (15)$$

where, $\hat{\Omega}$ is the rotation unit vector, $\rho = R/R_{LC}$, $\hat{\rho}$ is the radial unit vector, $b_0 = B/B$. The full expression for (15) is derived as equation (B13) in Appendix B.

To illustrate the asymmetry in θ , consider an orthogonal rotator with the inclination angle $\alpha = \pi/2$. Consider a ray in the 1–2 plane that contains the magnetic axis, with the rotation axis being perpendicular to the plane (Fig. 7). This is equivalent to setting

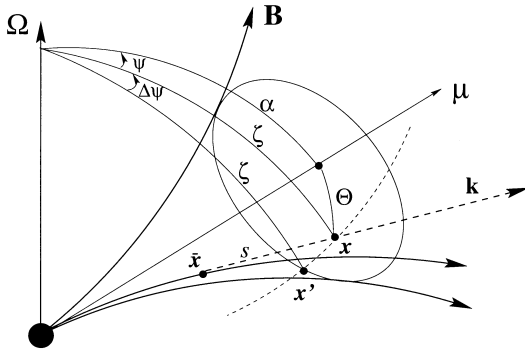


Figure 6. A rotating dipole. The inclination angle between Ω and the magnetic axis μ is α . A ray that starts at \bar{x} and propagates a distance s (in R_{LC}) crosses a field line that rotates from x' to x through an angle $\Delta\Psi = \Omega\Delta t = s$ where $\Delta t = |x - \bar{x}|/c = s/\Omega$.

$\zeta = \pi/2$ and $\Psi = \Theta$, where in deriving a general formalism for b we introduce the polar coordinates (R, ζ, Ψ) with respect to the rotation axis (cf. Appendix B). In Cartesian coordinates, with the three-axis in the direction of the angular velocity, Ω , one finds

$$b = (b'_1 \cos \Delta\Psi - b'_2 \sin \Delta\Psi, b'_2 \cos \Delta\Psi + b'_1 \sin \Delta\Psi, 0), \quad (16)$$

where equation (B19) from Appendix B with $b'_\perp = 1$ is used, $b'_1 = 3 \cos \Theta' \sin \Theta'/2A(\Theta')$, $b'_2 = (3 \cos^2 \Theta' - 1)/2A(\Theta')$, $\Theta' = \Theta + \Delta\Psi$ and $\Delta\Psi = \pm s$. If we assume the initial propagation direction to be in the bulk flow direction, \bar{b} , given by (15), we obtain

$$\bar{b} = \frac{1}{2A(\bar{\Theta})} \left(1 + \frac{\bar{\rho}}{2A(\bar{\Theta})} \sin \bar{\Theta} \right) \times \left[\frac{3}{2} \sin(2\bar{\Theta}) - 2\bar{\rho} \cos \bar{\Theta}, 3 \cos^2 \bar{\Theta} - 1 + 2\bar{\rho} \sin \bar{\Theta}, 0 \right], \quad (17)$$

where $\bar{\rho} = \bar{R}/R_{LC}$, $(\bar{R}, \bar{\Theta}, \bar{\Phi})$ are polar coordinates of \bar{x} . From (16) and (17) we can evaluate (14) for θ .

From (18) we see that b is independent of $\Delta\Psi$ only for straight field lines. In general, b is not symmetric with respect to the magnetic axis, because b is different for $\Delta\Psi > 0$ and for $\Delta\Psi < 0$. Fig. 8 shows plots of θ versus s with $\bar{\rho} = 0.1$. Fig. 9 shows that the asymmetry depends on the field-line colatitude angle Θ_* and the initial location $\bar{\rho}$. The asymmetry is reduced for decreasing Θ_* or $\bar{\rho}$. Similar plots with the initial direction being along the magnetic field-line tangential direction are shown in Figs 10 and 11.

5.2 Pulsars with asymmetric double-peak pulse profiles

A small group of pulsars have interpulses, that is, a small peak appears at an intermediate pulse phase between two main pulses (Manchester & Lyne 1977; Lyne & Manchester 1988). The separation between the main pulses and the interpulses ranges from 150° to about 180° . A good example is PSR 1549–4848 which has a separation of nearly 180° (Manchester, Han & Qiao 1998). In the two-pole model, the double-peak pulse is explained in terms of emission from the two opposite poles when a pulsar is an orthogonal rotator. Alternatively, the main pulse and the interpulse are interpreted as emissions from a wide, hollow cone from a single

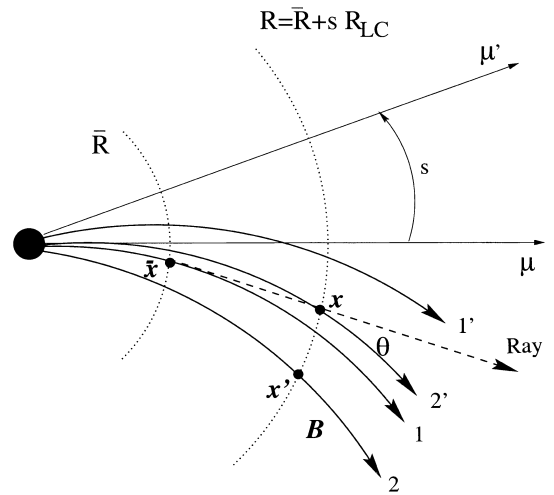


Figure 7. An orthogonal rotator with the rotation axis pointed to the reader. When the ray reaches to x , the field lines 1 and 2 rotate to 1' and 2' arcsec by an angle $\Omega\Delta t = s$ where $\Delta t = |x - \bar{x}|/c$. If there is no rotation, the ray always crosses the adjacent field lines with smaller colatitude angles.

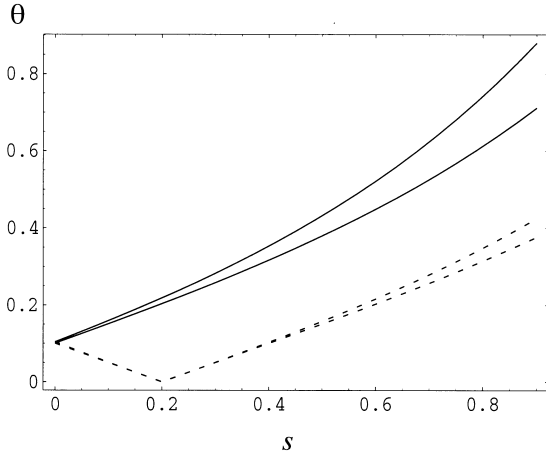


Figure 8. Crossing angle versus ray distance. The propagation direction is along the flow velocity. The solid curves are obtained with $\Delta\Psi > 0$, and the dashed curves with $\Delta\Psi < 0$. The starting point at $\bar{\rho} = \bar{R}/R_{LC} = 0.1$ on the field lines $\eta = (\sin\Theta_*/\sin\Theta_d)^2 = 1$ (the outer two curves), corresponding to the last open field line, 0.1 (the inner two curves).

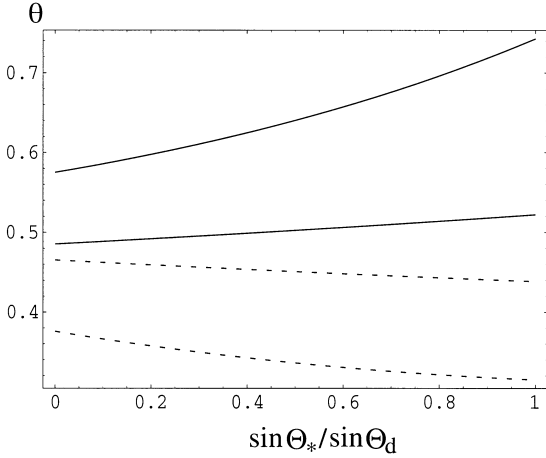


Figure 9. Crossing angle versus $\sin\Theta_*/\sin\Theta_d$. The solid curves are obtained with $\Delta\Psi > 0$, and the dashed curves with $\Delta\Psi < 0$. The outer and inner pair of curves are obtained with $\bar{\rho} = 0.1$ and 0.01 . The parameters are the same as in Fig. 8 but with $s = 0.8$.

pole (Manchester & Lyne 1977; Manchester 1996). We suggest the possibility that if the two components are emitted from a single wide conical beam, one of them tends to be suppressed because of the asymmetric cyclotron absorption.

Cyclotron absorption is pulse-phase dependent as a result of this asymmetry in propagation angle. This effect is especially important for emission from the cone defined by the last open field lines, where the propagation is most asymmetric. Such emission produces pulses with two peaks if the line of sight cuts across the hollow cone. In the observer's frame, the aberration increases by θ on one side of the cone, leading to greater absorption; on the other side of the cone the effect tends to decrease by θ and absorption is reduced. For the double peak pulse, the trailing pulse is more strongly affected by NCR than the leading pulse. In the case of marginal absorption in which $\tau < 1$ and the pulses are not completely destroyed by the cyclotron absorption, the trailing pulse should be considerably weaker than the leading. To estimate the asymmetry in intensity we assume the least affected peak has intensity $I_1 = I_0 \exp(-\tau_1)$ with τ_1 the optical

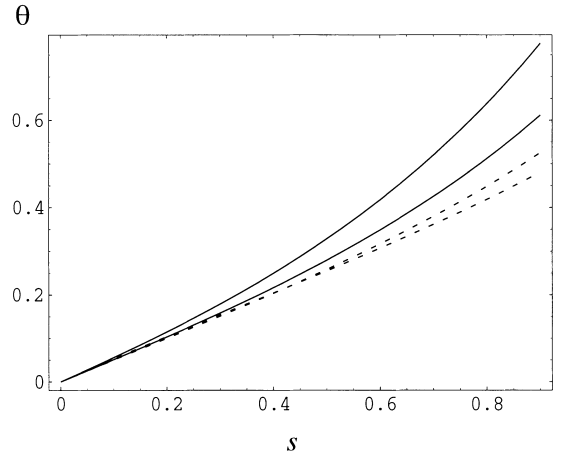


Figure 10. As in Fig. 8 with the initial propagation direction being along the magnetic field line tangential.

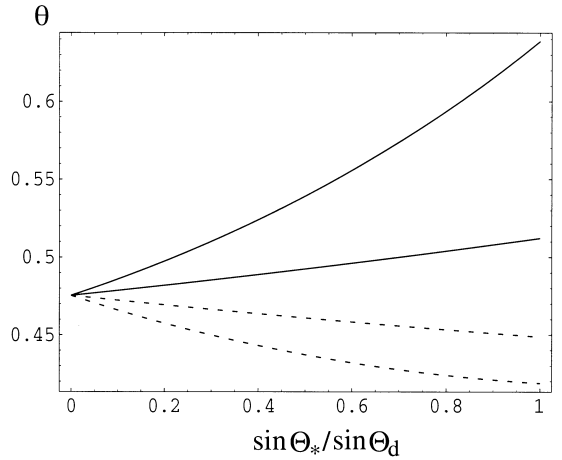


Figure 11. As in Fig. 9 with the initial propagation direction being along the magnetic field line tangential.

depth and I_0 the initial intensity. The intensity ratio of the leading to trailing peaks is given by

$$\frac{I_2}{I_1} = \exp\left[-\left(\frac{\theta_2^2}{\theta_1^2} - 1\right)\tau_1\right], \quad (18)$$

where θ_1 and θ_2 are the propagation angles of the leading and trailing radio beams (corresponding to the leading and lagging pulse components). The intensity ratio of the two peaks strongly depends on the optical depth of the least absorbed beam. From Figs 8 and 9, we have $(\theta_2/\theta_1)^2 = 6.3$. Assuming $\tau_1 = 0.5$, we have $I_2/I_1 \approx 0.05$. Therefore, one component has a much smaller intensity. Plots of I_2/I_1 against τ_1 are shown in Fig. 12. In some cases the weaker component is too weak to be observed. One possible example is the Vela pulsar, which has a double-peak pulse profile in X- and γ -ray emission but not in radio emission. The 'missing' interpulse may be a result of suppression by asymmetric cyclotron absorption.

In principle, the asymmetric cyclotron absorption effect allows us to distinguish whether the double peaks are caused by a nearly aligned rotator or an oblique rotator. A nearly aligned rotator can produce a wide separated double pulse profile with emission region located close to the PC. From the above discussion, for a smaller $\bar{\rho}$

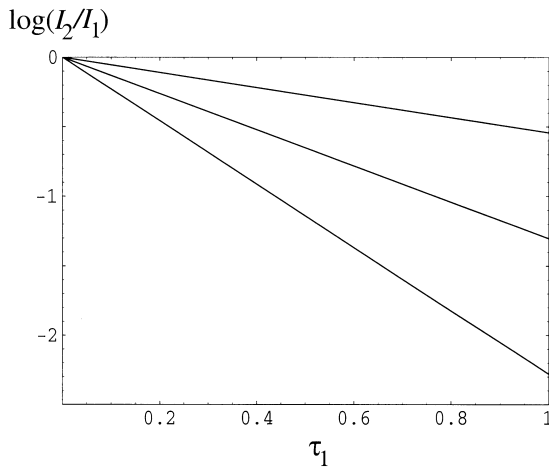


Figure 12. The intensity ratio of the first to second beams as a function of the optical depth τ_1 for $\theta_2/\theta_1 = 1.5, 2$ and 2.5 (from top to bottom).

and the inclination angle $\alpha \approx 0$, the propagation angle is approximately symmetric in the magnetic azimuth. Therefore, the cyclotron absorption of the two peaks is similar. For an oblique rotator, one requires that the emission can escape at a higher altitude corresponding to a large $\bar{\rho}$. In this case, we have very asymmetric absorption, i.e. the second peak is always subjected to more absorption.

From equations (7) or (10), the cyclotron absorption depends on frequency through the relationship $\tau \propto 1/\omega^{1/3}$. If waves with different frequencies are emitted at the same location, one expects the asymmetry between the two peaks to decrease with increasing frequency. However, if waves are emitted at different altitudes with different frequency, the intensity ratio may not depend strongly on frequency.

6 CONCLUSIONS AND DISCUSSION

We discuss cyclotron damping of pulsar radio emission inside the LC including the effect of a broad pair plasma distribution. Assuming an intrinsically relativistic distribution, the damping rate is calculated. It is shown that cyclotron absorption can occur for a large fraction of known pulsars. In general, there are two parameter regimes for NCR absorption: small angle propagation (including the special case of parallel propagation), $\theta < 1/\gamma$, and large angle propagation, $\theta > 1/\gamma$. In the former case, the resonance frequency is $\omega = 2\gamma\Omega_e \gg \Omega_e$, a condition that is not satisfied inside the LC for the majority of pulsars. It is shown that for the majority of pulsars, NCR damping occurs in the large propagation angle regime with the resonant frequency being $\omega = 2\Omega_e/\gamma\theta$. The waves that can be damped in the large propagation angle regime must have the superluminal parallel phase speed $z > 1$. This condition is satisfied in the pulsar magnetosphere because the relevant waves generated by a certain type of instability in the region with subluminal parallel phase speed $z < 1$ cross the light line $z = 1$, to have $z > 1$ as the propagation angle increases. Although radio emission is beamed initially in the direction of the particle velocity, because of the field line curvature the rays acquire a substantial angle with magnetic field lines as they propagate outwards.

Upon including rotation it is found that the propagation angle is non-axisymmetric with respect to the magnetic azimuthal angle. This asymmetry leads to pulse phase dependence of cyclotron

absorption. Asymmetric cyclotron absorption can be potentially observable for emission that originates from a wide cone of an oblique rotator. The class of pulsars that is favorable for detection of this effect are those with a double peak profile with a wide separation. For marginal absorption with $\tau \leq 1$, the second peak should be much weaker than the first because the former is subjected to the more severe absorption as the result of a larger propagation angle. In the single-pole model, pulsars with interpulses are interpreted as emission from a wide conical beam from a single pole. Thus a weaker intensity of one component, corresponding to the interpulse, can be caused by relatively more cyclotron absorption.

In discussing cyclotron absorption we have neglected differential absorption of waves with different polarizations (X mode and L–O mode). This approximation is valid for sufficiently underdense plasmas for which waves are considered as being transverse. If NCR occurs in the region where the plasma is moderately dense, X mode and L–O mode are subjected to differential absorption with one of these two modes tending to be preferentially absorbed. For some pulsars, this differential absorption can be important and can result in polarization features varying across a pulse profile, which is potentially observable.

So far, our discussion concentrates on cyclotron absorption inside the LC. The possibility that for very young normal pulsars and very fast MSPs cyclotron resonance occurs outside the LC cannot be excluded. However, the plasma conditions beyond the LC are qualitatively different from that inside the LC, with magnetic fields being dominantly toroidal, and the escaping rays should propagate at approximately a right angle to the field lines. A detailed discussion of cyclotron damping outside the LC will be given elsewhere.

ACKNOWLEDGMENTS

We thank Simon Johnston, Gia Machabeli, Dick Manchester, Shinpei Shibata for helpful discussion. The Australian Research Council (ARC) provided support.

REFERENCES

- Arons J., Barnard J. J., 1986, *ApJ*, 302, 120
- Barnard J. J., 1986, *ApJ*, 303, 280
- Barnard J. J., Arons J., 1986, *ApJ*, 302, 138
- Blandford R. D., Scharlemann E. T., 1976, *MNRAS*, 174, 59
- Blaskiewicz M., Cordes J., Wasserman I., 1991, *ApJ*, 370, 643
- Daugherty J. K., Harding A. K., 1982, *ApJ*, 252, 337
- Daugherty J. K., Harding A. K., 1983, *ApJ*, 273, 761
- Gedalin M., Melrose D. B., Gruman E., 1998, *Phys. Rev. E*, 57, 3399
- Gould D. M., Lyne A. G., 1998, *MNRAS*, 301, 235
- Han J. L., Manchester R. N., Xu R. X., Qiao G. J., 1998, *MNRAS*, 300, 373
- Hibschman J. A., Arons J., 2001, *ApJ*, 546, 382
- Kazbegi A. Z., Machabeli G. Z., Melikidze G. I., 1991, *MNRAS*, 253, 377
- Kennett M. P., Melrose D. B., Luo Q., 2001, *J. Plasma Phys.*, in press (KML)
- Lominadze D. G., Machabeli G. Z., Melikidze G. I., Pataraya A. D., 1986, *Sov. J. Plasma Phys.*, 12, 712
- Luo Q., Shibata S., Melrose D. B., 2000, *MNRAS*, 318, 943
- Lyne A. G., Manchester R. N., 1988, *MNRAS*, 234, 477
- Lyubarskii Y. E., Petrova S. A., 1998, *A&A*, 337, 433
- Lyutikov M., Blandford R., Machabeli G. Z., 1999, *MNRAS*, 305, 338
- Machabeli G. Z., Usov V. V., 1979, *Sov. Astron. Lett.*, 5, 238
- McKinnon M. M., 1997, *ApJ*, 475, 763
- McKinnon M. M., Stinebring D. R., 1998, *ApJ*, 502, 883
- Manchester R. N., 1996, in Johnston S. et al., eds, *ASP Conf. Ser. Vol. 105*,

- Pulsars: Problems & Progress. Astron. Soc. Pac., San Francisco, p. 193
- Manchester R. N., Lyne A. G., 1977, MNRAS, 181, 761
- Manchester R. N., Han J., Qiao G., 1998, MNRAS, 295, 280
- Melrose D. B., 1979, Aust J. Phys., 32, 61
- Melrose D. B., 2000, in Kramer M., Wex N., eds, ASP Conf. Ser. Vol. 202, Pulsar Astronomy – 2000 and Beyond, Astron. Soc. Pac., San Francisco, p. 721
- Melrose D. B., Gedalin M. E., 1999, ApJ, 521, 351
- Mikhailovskii A. B., 1979, Sov. Astron. Lett., 5, 323
- Mikhailovskii A. B., Onishchenko O. G., Suramlishvili G. I., Sharapov S. E., 1982, Sov. Astron. Lett., 8, 369
- Shibata S., Miyazaki J., Takahara F., 1998, MNRAS, 295, L53
- Shitov Yu. P., 1985, Sov. Astron., 29, 33
- Weatherall J. C., 1994, ApJ, 428, 261

APPENDIX A: ABSORPTION COEFFICIENT

A general formula for calculation of the (temporal) absorption rate is given by

$$\Gamma = -2i\omega R_E K^A, \quad (A1)$$

where $K^A = e_i^* K_{ij}^A e_j$, the dielectric tensor, is separated into its antihermitian and hermitian components, $K_{ij} = K_{ij}^A + K_{ij}^H$, e is the polarization vector and R_E is the ratio of electric to total energy in the wave, given by (Melrose 1986)

$$R_E = \frac{\omega}{\partial(\omega^2 K^H)/\partial\omega}. \quad (A2)$$

In both equations (A1) and (A2), dispersion of a particular wave mode is specified.

For the X mode, the polarization vector is $e_X = (0, i, 0)$, so that the only relevant component of the dielectric tensor is (e.g. Lominadze et al. 1986; Kazbegi et al. 1991; Melrose & Gedalin 1999; KML)

$$K_{22} = 1 - \frac{\omega_p^2}{\omega^2} \int \frac{du_{\parallel}}{\gamma} F(u_{\parallel}) (\omega - k_{\parallel} v_{\parallel}) \times \left(\frac{1}{\omega - k_{\parallel} v_{\parallel} - \Omega_e/\gamma} + \frac{1}{\omega - k_{\parallel} v_{\parallel} + \Omega_e/\gamma} \right), \quad (A3)$$

where $u = \gamma\beta$ and $F(u)$ is the plasma distribution function which is normalized to unity. The antihermitian part is therefore

$$K^A = K_{22}^A = i\pi \frac{\omega_p^2}{\omega^2} \int \frac{du_{\parallel}}{\gamma} F(u_{\parallel}) \frac{\Omega_e}{\gamma} \times [\partial(\omega - k_{\parallel} v_{\parallel} - \Omega_e/\gamma) - \partial(\omega - k_{\parallel} v_{\parallel} + \Omega_e/\gamma)] = i\pi \frac{\omega_p^2 \Omega_e}{\omega^2} \left[\frac{\gamma - F(u_-)}{|k_{\parallel} c - \beta_- \gamma - \Omega_e|} - \frac{\gamma + F(u_+)}{|k_{\parallel} c + \beta_+ \gamma + \Omega_e|} \right], \quad (A4)$$

where the integration is carried out using $du_{\parallel} \approx \gamma^3 d\beta_{\parallel}$, ω_p is the pair-plasma frequency, u_+ and u_- satisfy respectively the two resonance conditions and $\omega - k_{\parallel} v_{\parallel} \pm \Omega_e/\gamma = 0$. The first term in the square brackets corresponds to NCR, which gives rise to the cyclotron damping. The second term is ACR that results in cyclotron instability (e.g. Machabeli & Usov 1979; Kazbegi et al. 1991).

Considering waves with $z > 1$ in NCR, with particles with γ_+ given by (4), we have

$$K^A \approx i\pi \frac{\omega_p^2}{\omega^2} F(u_+), \quad (A5)$$

where $\gamma_{\pm} = 1/(1 - \beta_{\pm}^2)^{1/2}$, $u_{\pm} = \gamma_{\pm} \beta_{\pm}$ and β_{\pm} are given by

equation (1). The approximation in equation (A5) is valid for $\omega \ll \gamma_{\pm} \Omega_e$. For $|n - 1| \ll \theta^2/2 \ll 1$, we have

$$\gamma_+ = 2\Omega_e/\omega\theta^2, \quad (A6)$$

with θ as the propagation angle relative to the magnetic field. Assuming $R_E = 1/2$, one obtains the absorption coefficient (5). Using equation (A6), equation (5) reduces to equation (1) in Blandford & Scharlemann (1976).

For the L–O mode the polarization vector is $e_{L-O} = (e_1, 0, e_3)$. Then we have

$$K_{L-O}^A = |e_1|^2 K_{11}^A + (e_1^* e_3 + e_1 e_3^*) K_{13}^A + |e_3|^2 K_{33}^A, \quad (A7)$$

where K_{11}^A is identical with K_{22}^A . For $\theta \ll 1$, the first term dominates. Thus we have $\Gamma_{L-O} \approx \Gamma_X$.

APPENDIX B: PROPAGATION ANGLE RELATIVE TO THE MAGNETIC FIELD LINE

We consider a photon propagating along a straight line in a rotating dipole magnetic field. The photon is assumed to be emitted at a point \bar{x} propagating along a direction \bar{b} . We are interested in the angle, θ , between the propagation direction and the local direction of the magnetic field, b , at x at a distance s along the photon's path.

We introduce Cartesian coordinates with the three-axis along the direction of the angular velocity, Ω . In these coordinates, the point x is given by

$$x_1 = \bar{x}_1 + s\bar{b}_1, \quad x_2 = \bar{x}_2 + s\bar{b}_2, \quad x_3 = \bar{x}_3 + s\bar{b}_3, \quad (B1)$$

and the angle θ is determined by

$$\cos \theta = \bar{b}_1 b_1 + \bar{b}_2 b_2 + \bar{b}_3 b_3. \quad (B2)$$

We also introduce the polar coordinates (R, Θ, Φ) relative to the magnetic axis, and the polar coordinates (R, ζ, Ψ) relative to the rotation axis. The equation for a dipole field line is

$$R = R_* \left(\frac{\sin \Theta}{\sin \Theta_*} \right)^2, \quad (B3)$$

where $0 \leq \Theta_* \leq \Theta_d = (R_*/R_{LC})^{1/2}$ is the colatitude on the surface of the star. The direction of a dipole field line is given by

$$b_0 = \frac{1}{A} (e_R \cos \Theta + e_{\Theta} \sin \Theta/2), \quad (B4)$$

where $A = [1 - (3/4) \sin^2 \Theta]^{1/2}$, and where e_R , e_{Θ} and e_{Φ} are unit vectors along the polar directions relative to the magnetic axis. The Cartesian coordinates of these unit vectors can be derived by first expressing them in terms of polar coordinates relative to the rotation axis, that is, $e_R = e_R$, $e_{\Theta} = e_{\zeta} \cos \delta + e_{\Psi} \sin \delta$ and $e_{\Phi} = e_{\zeta} \sin \delta - e_{\Psi} \cos \delta$ with $\sin \delta = \sin \alpha \sin \Psi / \sin \Theta$. Then, using

$$e_R = (\sin \zeta \sin \Psi, \sin \zeta \cos \Psi, \cos \zeta), \quad (B5)$$

$$e_{\zeta} = (\cos \zeta \sin \Psi, \cos \zeta \cos \Psi, -\sin \zeta), \quad (B6)$$

and

$$e_{\Psi} = (\cos \Psi, \sin \Psi, 0), \quad (B7)$$

we have

$$e_{\Theta} = (\cos \zeta \sin \Psi \cos \delta + \cos \Psi \sin \delta, \cos \zeta \cos \Psi \cos \delta + \sin \Psi \sin \delta, -\sin \zeta \cos \delta), \quad (B8)$$

$$e_{\Phi} = (\cos \zeta \sin \Psi \sin \delta - \cos \Psi \cos \delta, \cos \zeta \cos \Psi \sin \delta - \sin \Psi \cos \delta, -\sin \zeta \sin \delta). \quad (B9)$$

Then equation (B4) in Cartesian coordinates is

$$\begin{aligned} \mathbf{b}_0 = & \frac{1}{A} \left[\cos \Theta \sin \zeta \sin \Psi + \frac{1}{2} \sin \Theta (\cos \zeta \cos \delta \sin \Psi + \sin \delta \cos \Psi), \right. \\ & \times \cos \Theta \sin \zeta \cos \Psi + \frac{1}{2} \sin \Theta (\cos \zeta \cos \delta \cos \Psi - \sin \delta \sin \Psi), \\ & \left. \times \cos \Theta \cos \zeta - \frac{1}{2} \sin \Theta \cos \delta \sin \zeta \right]. \end{aligned} \quad (\text{B10})$$

The direction of emission of the photon is assumed to be along the flow direction of the particles. This direction differs from the direction tangent to the field lines as a result of the corotational velocity, $\boldsymbol{\Omega} \times \mathbf{R}$, at a point \mathbf{R} . The aberration caused by rotation is given by (e.g. Blaskiewicz, Cordes & Wasserman 1991; Hibsman & Arons 2000)

$$\Delta \mathbf{b} = \frac{1}{c} [\boldsymbol{\Omega} \times \mathbf{R} - (\boldsymbol{\Omega} \times \mathbf{R}) \cdot \mathbf{b}_0 \mathbf{b}_0]. \quad (\text{B11})$$

In Cartesian coordinates, one has $\hat{\boldsymbol{\Omega}} \times \hat{\mathbf{R}} = (-\sin \zeta \cos \Psi, \sin \zeta \sin \Psi, 0)$ and

$$(\hat{\boldsymbol{\Omega}} \times \hat{\mathbf{R}}) \cdot \mathbf{b}_0 = -\frac{1}{2A} \sin \zeta \sin \alpha \sin \Psi. \quad (\text{B12})$$

From (B10) and (B11) we obtain the flow direction as $\mathbf{b}_v = \mathbf{b}_0 + \Delta \mathbf{b}$ with

$$\begin{aligned} \mathbf{b}_v = & \left\{ \frac{1}{A} \left(1 + \frac{\rho}{2A} \sin \zeta \sin \alpha \sin \Psi \right) [\cos \Theta \sin \zeta \sin \Psi \right. \\ & \left. + \frac{1}{2} \sin \Theta (\cos \zeta \cos \delta \sin \Psi + \cos \Psi \sin \delta)] - \rho \sin \zeta \cos \Psi, \right. \\ & \frac{1}{A} \left(1 + \frac{\rho}{2A} \sin \zeta \sin \alpha \sin \Psi \right) [\cos \Theta \sin \zeta \cos \Psi \\ & \left. + \frac{1}{2} \sin \Theta (\cos \zeta \cos \delta \cos \Psi - \sin \Psi \sin \delta)] + \rho \sin \zeta \sin \Psi, \right. \\ & \left. \frac{1}{A} (\cos \Theta \cos \zeta - \frac{1}{2} \sin \Theta \cos \delta \sin \zeta) \right\}. \end{aligned} \quad (\text{B13})$$

The aberration effect is reflected by the presence of the terms that depend on ρ .

To calculate equation (B2) we may assume $\bar{\mathbf{b}}$ to be along the flow direction. Thus, $\bar{\mathbf{b}}$ is given by (B13), with all the relevant quantities being replaced with barred quantities.

To derive the local tangential vector of the magnetic field lines at \mathbf{x} , we need to consider a point \mathbf{x}' on a rotation curve that passes through \mathbf{x} . The locations of these two points differ by a rotation angle $\Omega \Delta t = \Omega s/c$. Then, the local tangential direction, \mathbf{b} , can be obtained by first deriving the local tangential direction, \mathbf{b}' , at \mathbf{x}' , and then rotating \mathbf{b}' by an angle $\Omega \Delta t$. We assume \mathbf{b}' to be the tangential direction of the field line at \mathbf{x}' . Thus, this vector is given by (B10) with all the relevant angles being for the point \mathbf{x}' (hence all the relevant angles are primed). Let $\Delta \Psi = \Omega \Delta t$. Thus, Θ' at \mathbf{x}' is determined by

$$\begin{aligned} \cos \Theta' = & \cos \alpha \cos \zeta + \sin \alpha \sin \zeta \cos(\Psi + \Delta \Psi) \\ = & \frac{1}{R} [x_3 \cos \alpha + (x_2 \cos \Delta \Psi - x_1 \sin \Delta \Psi) \sin \alpha], \end{aligned} \quad (\text{B14})$$

with $R = (x_1^2 + x_2^2 + x_3^2)^{1/2}$. The azimuthal angle Φ' is obtained by

$$\cos \Phi' = \frac{\cos \alpha - \cos \zeta \cos \Theta'}{\sin \zeta \sin \Theta'}, \quad (\text{B15})$$

$$\sin \zeta = \left(\frac{x_1^2 + x_2^2}{x_1^2 + x_2^2 + x_3^2} \right)^{1/2}, \quad (\text{B16})$$

and

$$\cos \zeta = \frac{x_3}{(x_1^2 + x_2^2 + x_3^2)^{1/2}}, \quad (\text{B17})$$

where (x_1, x_2, x_3) are given by (B1) together with (A9)–(B11). Then, \mathbf{b} is derived by rotating \mathbf{b}' by an angle $\Delta \Psi$ with respect to $\boldsymbol{\Omega}$, that is,

$$\mathbf{b} = (b'_\perp \sin(\Psi'_b - \Delta \Psi), b'_\perp \cos(\Psi'_b - \Delta \Psi), b'_3), \quad (\text{B18})$$

where $\tan \Psi'_b = b'_1/b'_2$ and

$$\begin{aligned} b'_\perp = & (b_1'^2 + b_2'^2)^{1/2} = \frac{1}{A} [\cos^2 \Theta' \sin^2 \zeta \\ & + \frac{1}{4} \sin^2 \Theta' (\cos^2 \zeta + \sin^2 \zeta \sin^2 \delta) \\ & + \frac{1}{4} \sin(2\Theta') \sin(2\zeta) \sin(2\Psi) \cos \delta]^{1/2}, \end{aligned} \quad (\text{B19})$$

$$b'_3 = \cos \Theta' \cos \zeta - \frac{1}{2} \sin \Theta' \cos \delta \sin \zeta. \quad (\text{B20})$$

Equation (B10) (or equation B13) can reduce to the non-rotation approximation by setting $\zeta \rightarrow \Theta, \delta \rightarrow 0, \Psi \rightarrow \pi/2$ and neglecting the terms with ρ . Thus, we have

$$\mathbf{b}_0 = \frac{1}{2A} (3 \cos \Theta \sin \Theta, 0, 3 \cos^2 \Theta - 1), \quad (\text{B21})$$

where the three-axis is along $\boldsymbol{\mu}$. Assume that $\bar{\mathbf{b}} = \bar{\mathbf{b}}_0$ takes the form (B21) with $\Theta \rightarrow \bar{\Theta}$. The polar angle $\bar{\Theta}$ can be expressed in terms of the radial distance using $\sin \bar{\Theta} = (\eta \bar{\rho})^{1/2}$ with $\bar{\rho} < 1$. Then, the propagation angle in the non-rotation approximation is

$$\begin{aligned} \cos \theta = & \bar{\mathbf{b}}_0 \cdot \mathbf{b}_0 = \frac{1}{AA} \{ 9(1 - \eta \bar{\rho})^{1/2} (\eta \bar{\rho})^{1/2} \cos \Theta \sin \Theta \\ & + (2 - 3\eta \bar{\rho})(3 \cos^2 \Theta - 1) \}, \end{aligned} \quad (\text{B22})$$

$$\bar{A} = (1 - \frac{3}{4} \eta \bar{\rho})^{1/2}. \quad (\text{B23})$$

$$\tan \Theta = \frac{s \bar{b}_1 + \eta^{-1} (\eta \bar{\rho})^{3/2}}{s \bar{b}_3 + \bar{\rho} (1 - \eta \bar{\rho})^{1/2}}. \quad (\text{B24})$$

Equation (B24) is symmetric with respect to the magnetic azimuth.

This paper has been typeset from a $\text{\TeX}/\text{\LaTeX}$ file prepared by the author.